Theoretical studies of the decay chain of the isotopes $^{298,299}120$

C. Nithya [1,*] and K. P. Santhosh [2,3]

[1]*Department of Physics, The Zamorin's Guruvayurappan College, Calicut 673014, Kerala, India*

[2]*Department of Physics, University of Calicut, Thenhipalam 673635, Kerala, India*

[3]*School of Pure and Applied Physics, Kannur University, Swami Anandatheertha Campus, Payyanur 670327, Kerala, India*

(Received 27 May 2023; accepted 29 June 2023; published 17 July 2023)

The α-decay properties of the two isotopes $^{298}120$ and $^{299}120$ are studied in the paper. The decay energies are calculated using five different mass tables and are compared with the experimental results. The discrepancy between experimental and the calculated Q value is found to be minimum while using the purely microscopic Hartree-Fock-Bardeen-Cooper-Schrieffer mass model. The α-decay half-lives of the isotopes are calculated using the Coulomb and proximity potential model for deformed nuclei and other theoretical formalisms. The sensitivity of half-lives to the Q value is evident from the study. The length of the decay chain for the isotopes is found out by comparing the α half-lives with the corresponding spontaneous fission half-lives calculated using the shell-effect-dependent formula. The paper shows that the isotopes $^{298}120$ and $^{299}120$ will decay via the 4α chain followed by spontaneous fission. The predicted half-lives are well within the experimental limit.

DOI: 10.1103/PhysRevC.108.014606

I. INTRODUCTION

The experimental and theoretical studies of superheavy nuclei have achieved significant progress in recent years. The search for superheavy nuclei is on track after the prediction of magic island or island of stability [1–5]. With the advancement of latest experimental techniques, elements up to $Z = 118$ (Og) has been synthesized yet. Two types of fusion reactions, namely, the cold fusion reaction [6] and the hot fusion reaction [7] are used for the synthesis of superheavy elements.

Experiments to synthesize the isotopes of $Z = 119$ and 120 is in progress in different laboratories. Attempts to synthesize the isotopes $^{298,299}120$ was performed by Oganessian *et al.* in 2009 [8]. The fusion reaction of ^{244}Pu and ^{58}Fe was used to synthesize the compound nucleus $^{302}120$. The maximum yield of the evaporation residues is expected for the $3n$- and $4n$-evaporation channels that result in the formation of the isotopes $^{299}120$ and $^{298}120$, respectively. Different approaches to synthesize the isotopes of $Z = 120$ has been investigated [9–14] following the experiment of Oganessian *et al.* [8]. However, none of these experiments provides valid evidences for the synthesis of new element.

Along with the experimental progress, different theoretical studies are also performed to analyze the properties of the isotopes with $Z = 120$ [15–26]. Since superheavy nuclei are identified through their decay chain, the studies on decay properties have prime importance in the superheavy region. The main decay modes of superheavy nuclei are α decay and spontaneous fission. The α-decay chain can be considered as the experimental signature for the identification of new elements.

In the present paper, the α-decay chains of the isotopes $^{298,299}120$ have been studied using different mass tables [27–31]. The well known Coulomb and proximity potential model for deformed nuclei (CPPMDN) [32] is used to study the alpha α-ecay half-lives. The half-lives calculated using CPPMDN is compared with the values computed using several other theoretical models [33–39] as well as with the experimental results [8]. The decay modes of the isotopes are predicted by comparing the α half-lives with the spontaneous fission half-lives calculated using the shell effect-dependent formula [40].

The paper is organized as follows: Sec. II deals with the description of CPPMDN. The results and discussions are included in Sec. III. Section IV gives the summary of the entire paper.

II. THE COULOMB AND PROXIMITY POTENTIAL MODEL FOR DEFORMED NUCLEI

The CPPMDN is one of the successful models for the description of different decay mechanisms, such as α decay and cluster decay. In the model, the deformation energy barrier is constructed by modifying the Coulomb repulsion between the fragments and the attractive nuclear proximity potential up to the contact of the fragments and continuing beyond contact by an interpolation to the configuration of parent nucleus. Even though such arbitrary perceptions are used while developing the model, it can be effectively used for predicting the decay half-lives. One of the weaknesses of the model CPPMDN is the approximation of the Coulomb potential for one-body shapes. It is a polynomial, but there is no physics contained in it.

*nithyachandrann@gmail.com

In CPPMDN, the interacting potential between two nuclei is taken as the sum of deformed Coulomb potential, deformed two term proximity potential and centrifugal potential for both the touching configuration and the separated fragments. It is given by

$$V = V_C(r,\theta) + V_{P2}(r,\theta) + \frac{\hbar^2 \ell(\ell+1)}{2\mu r^2}, \tag{1}$$

where $V_c(r,\theta)$ is the Coulomb interaction between the two deformed and oriented nuclei, $V_{P2}(r,\theta)$ is the two-term proximity potential, ℓ represents the angular momentum, and μ represents the reduced mass.

The Coulomb interaction between the two deformed and oriented nuclei [41], $V_c(r,\theta)$,with higher multipole deformations [42,43] is given as

$$\begin{aligned} V_C(r,\theta) = {} & \frac{Z_1 Z_2 e^2}{r} + 3Z_1 Z_2 e^2 \\ & \times \sum_{\lambda=2,3,4;i=1,2} \frac{1}{2\lambda+1} \frac{R_{0i}^{\lambda}}{r^{\lambda+1}} Y_{\lambda}^{(0)}(\alpha_i) \\ & \times \left[\beta_{\lambda i} + \frac{4}{7} \beta_{\lambda i}^2 Y_{\lambda}^{(0)}(\alpha_i) \delta_{\lambda,2} \right]. \end{aligned} \tag{2}$$

Here, Z_1 and Z_2 are the atomic numbers of the daughter and emitted cluster, "r" is the distance between fragment centers and

$$R_i(\alpha_i) = R_{0i}\left[1 + \sum_{\lambda=2,3,4} \beta_{\lambda i} Y_{\lambda}^{(0)}(\alpha_i) \right], \tag{3}$$

where $R_{0i} = 1.28A_i^{1/3} - 0.76 + 0.8A_i^{-1/3}$. Here, α_i is the angle between the radius vector and symmetry axis of the ith nuclei (see Fig. 1 of Ref. [42]). The magnitude of the quadrupole-quadrupole interaction term, which is proportional to $\beta_{21}\beta_{22}$, is very small because of its short-range character, as compared to the other terms in the expression for deformed Coulomb potential [Eq. (2)]. The deformation values are taken from the recent mass table of Moller *et al.* [27].

The two-term proximity potential for interaction between a deformed and spherical nucleus given by Baltz and Bayman [44] is as follows:

$$\begin{aligned} V_{P2}(r,\theta) = {} & 2\pi \left[\frac{R_1(\alpha) R_C}{R_1(\alpha) + R_C + S} \right]^{1/2} \left[\frac{R_2(\alpha) R_C}{R_2(\alpha) + R_C + S} \right]^{1/2} \\ & \times \left\{ \left[\varepsilon_0(S) + \frac{R_1(\alpha) + R_C}{2R_1(\alpha) R_C} \varepsilon_1(S) \right] \right. \\ & \left. \times \left[\varepsilon_0(S) + \frac{R_2(\alpha) + R_C}{2R_2(\alpha) R_C} \varepsilon_1(S) \right] \right\}^{1/2}, \end{aligned} \tag{4}$$

where θ is the angle between the symmetry axis of the deformed nuclei and the line joining the centers of the two interacting nuclei, and α corresponds to the angle between the radius vector and the symmetry axis of the nuclei (see Fig. 5 of Ref. [44]). $R_1(\alpha)$ and $R_2(\alpha)$ are the principal radii of curvature of the daughter nuclei, R_C is the radius of the spherical cluster, S is the distance between the surfaces along the straight line connecting the fragments, and $\varepsilon_0(S)$ and $\varepsilon_1(S)$ are the one-dimensional slab-on-slab function.

For the prescission (overlap) region, simple power-law interpolation [45] has been used. The potential for the internal part of the barrier is given as

$$V = a_0(L - L_0)^n \text{ for } z < 0, , \tag{5}$$

here $L = z + 2C_1 + 2C_2$ fm and $L_0 = 2C$ fm, where C, C_1 and C_2 are the Süsmann central radii of parent nuclei, daughter nuclei and emitted cluster, respectively. The constants a_0 and n are determined by the smooth matching of the two potentials at the touching point.

The barrier penetrability P using the one-dimensional Wentzel-Kramers-Brillouin (WKB) approximation is as follows:

$$P = \exp\left\{ -\frac{2}{\hbar} \int_a^b \sqrt{2\mu(V-Q)}\, dz \right\}. \tag{6}$$

Here, the mass parameter is replaced by $\mu = mA_1A_2/A$, where m is the nucleon mass and A_1, A_2 are the mass numbers of daughter and emitted cluster, respectively. V represents the interacting potential between two nuclei. The turning points "a" and "b" are determined from the equation $V(a)$=$V(b)$=Q, where Q is the energy released.

The half-life of nuclei, which decay through α emission can be calculated by means of WKB approximation. The α-decay half-lives can be obtained using

$$T_{1/2} = \left(\frac{\ln 2}{\lambda} \right) = \left(\frac{\ln 2}{\nu P} \right), \tag{7}$$

where λ is the decay constant, ν is the assault frequency, and P is the barrier penetrability. The assault frequency ν can be calculated as

$$\nu = \left(\frac{\omega}{2\pi} \right) = \left(\frac{2E_v}{h} \right). \tag{8}$$

Here, E_v is the empirical vibration energy, which is given by [46]

$$E_v = Q\left\{ 0.056 + 0.039 \exp\left[\frac{(4 - A_2)}{2.5} \right] \right\} \text{ for } A_2 \geqslant 4. \tag{9}$$

The α particle vibrates in a harmonic-oscillator potential with a frequency ω, which depends on the vibrational energy E_v. We can identify this frequency as the assault frequency υ, and the expression for the empirical vibration energy E_v is used only for finding the assault frequency υ.

III. RESULTS AND DISCUSSION

Z = 120 is one of the elements, which is likely to be identified in the near future. A large number of theoretical and experimental studies are being performed in order to identify and study the properties of $Z = 120$. Among the isotopes of this element, nuclei with $A = 298$ and $A = 299$ will demand special attention. These are the two isotopes reported by Oganessian *et al.* [8] using the ^{244}Pu(^{58}Fe, xn)$^{302-x}$120 reaction in 2009.

In the present paper, an extensive study on the α-decay chains of these isotopes has been performed using different

mass models and different empirical formulas. The calculation of Q value plays an important role in the correct estimation of decay half-lives. For calculating the Q values, different mass tables are available in literature [27–31,47–50]. Half-lives are particularly sensitive to decay energies. An uncertainty of 1 MeV in the calculation of Q value will lead to several orders of uncertainty in predicting the decay half-lives. So it is very important to choose an accurate mass model in order to make reliable predictions of Q values and, hence, the half-lives. In this paper, we have chosen five different mass tables [27–31], which have already been proved to be the best choices [51,52] for calculating the decay energies in superheavy region. We have used the equation,

$$Q = \Delta M_p - (\Delta M_\alpha + \Delta M_d) + k\left(Z_p^\varepsilon - Z_d^\varepsilon\right). \tag{10}$$

Here ΔM_p, ΔM_d, and ΔM_α represent the mass excess of the parent, daughter, and the α particle respectively. The electron screening effect on the energy of α particle is included by adding the term $k(Z_p^\varepsilon - Z_d^\varepsilon)$ in Eq. (10). The term kZ^ε is the total binding energy of Z electrons in the atom. Here, $k = 8.7$ eV and $\varepsilon = 2.517$ for nuclei with $Z \geqslant 60$ and $k = 13.6$ eV and $\varepsilon = 2.408$ for nuclei with $Z < 60$ [53,54]. The Q value must be positive for α decay to occur.

For obtaining the mass excess values we have used finite range droplet model (FRDM) [27], the mass table of Koura *et al.* (KTUY) [28],the Weizsäcker-Skyrme formulas with radial basis function (WS4+RBF) [29], Hartree-Fock-BSC model (HFBCS) [30], and the nuclear Thomas and Fermi model (TFM) [31]. Among these, FRDM [27], WS3+RBF [29], and TFM [31] are macroscopic-microscopic models and HFBCS [30] is a pure microscopic model. The mass table of Koura *et al.* [28] presents a nuclidic mass formula composed of a gross term, an even-odd term, and a shell term.

After the calculation of the decay energy, the next step is to calculate the α half-lives. The CPPMDN [32] is used for calculating the α half-lives. The half-lives are calculated using all the Q values obtained with different mass tables. Along with CPPMDN, we have also used the analytical formula of Royer [33], the universal curve (UNIV) [34,35], the modified Brown formula (MBrown) [36], the formula of Akrawy and Poenaru (AP) [37], and the Viola-Seaborg semiempirical mass formula (VSS) [38,39] for calculating the decay half-lives.

The analytical formula of Royer [33] developed by applying a fitting procedure on the α emitters is as follows:

$$\log_{10}[T_{1/2}(s)] = a + bA^{1/6}\sqrt{Z} + \frac{cZ}{\sqrt{Q}}, \tag{11}$$

where A and Z represent the mass and charge numbers of the parent nuclei. The constants a, b, and c are given as

$$\begin{array}{lllll} a = -25.31, & b = -1.1629, & c = 1.5864, & \text{for} & Z = \text{even} \quad N = \text{even} \\ a = -26.65, & b = -1.0859, & c = 1.5848, & \text{for} & Z = \text{even} \quad N = \text{odd} \\ a = -25.68, & b = -1.1423, & c = 1.5920, & \text{for} & Z = \text{odd} \quad N = \text{even} \\ a = -29.48, & b = -1.1130, & c = 1.6971, & \text{for} & Z = \text{odd} \quad N = \text{odd} \end{array}. \tag{12}$$

The UNIV curve developed by Poenaru *et al.* [34,35] for calculating the α-decay half-lives is expressed as

$$\log_{10}[T_{1/2}(s)] = -\log_{10}P_S - \log_{10}S + [\log_{10}(\ln 2) - \log_{10}\nu]. \tag{13}$$

Here, υ is the frequency of assaults on the barrier per second, S is the preformation probability of the cluster at the nuclear surface, and P_S is the quantum penetrability of the external potential barrier. The penetrability of the potential barriers P_S is given by

$$-\log_{10}P_S = 0.22873(\mu_A Z_d Z_e R_b)^{1/2} \times [\arccos\sqrt{r} - \sqrt{r(1-r)}], \tag{14}$$

where $r = R_t/R_b$, $R_t = 1.2249(A_d^{1/3} + A_e^{1/3})$ fm, and $R_b = 1.43998 Z_d Z_e/Q$ fm. The decimal logarithm of the preformation factor S is as follows:,

$$\log_{10}S = -0.598(A_e - 1). \tag{15}$$

The additive constant for even-even nuclei is as follows:

$$c_{ee} = [-\log_{10}\nu + \log_{10}(\ln 2)] = -22.16917. \tag{16}$$

The modified Brown formula with an additional hindrance term depending on parity [36] is given by

$$\log_{10}[T_{1/2}(s)] = a\frac{Z^b}{\sqrt{Q}} + c + h^{mB1}. \tag{17}$$

The constants are $a = 13.0705$, $b = 0.5182$, and $c = -47.8867$. The hindrance term is given by, $h_{e-e}^{mB1} = 0$, $h_{o-e}^{mB1} = 0.6001$, $h_{e-o}^{mB1} = 0.466$, and $h_{o-o}^{mB1} = 0.8200$.

Akrawy and Poenaru [37] modified the Royer formula [33] by introducing $I = (N-Z)/A$ and is given as

$$\log_{10}[T_{1/2}(s)] = a + bA^{1/6}\sqrt{Z} + \frac{cZ}{\sqrt{Q}} + dI + eI^2. \tag{18}$$

The constants for different combinations of N and Z are as follows: $a = -26.322\,79$, $b = -1.159\,85$, $c = 1.592\,27$, $d = 12.060\,60$, and $e = -41.663\,28$ for even-even nuclei. $a = -24.407\,18$, $b = -1.232\,00$, $c = 1.654\,92$, $d = -31.862\,94$, and $e = 159.776\,82$ for even-odd nuclei. $a = -31.792\,48$, $b = -1.076\,36$, $c = 1.753\,54$, $d = -2.226\,27$, and $e = 0.393\,78$ for odd-even nuclei. $a = -26.278\,96$, $b = -1.201\,30$, $c = 1.659\,06$, $d = -10.084\,11$, and $e = 67.597\,28$ for odd-odd nuclei.

The phenomenological formula of Viola and Seaborg [38] with constants determined by Sobiczewski *et al.* [39]

TABLE I. Calculated values of α-decay energies and half-lives for the isotopes in the decay chain of $^{298}120$ using five different mass models and six different theoretical formalisms, respectively.

		$T^{\alpha}_{1/2}$ (s)					
Parent Nuclei	Q_{α} (MeV)	CPPMDN	Royer	UNIV	MBrown	AP	VSS
$^{298}120$	13.297[a]	7.938×10^{-06}	9.394×10^{-07}	6.809×10^{-07}	3.819×10^{-06}	1.020×10^{-06}	1.478×10^{-06}
	11.687[b]	3.491×10^{-02}	2.837×10^{-03}	1.334×10^{-03}	2.588×10^{-03}	3.174×10^{-03}	4.564×10^{-03}
	13.039[c]	1.436×10^{-05}	3.068×10^{-06}	2.059×10^{-06}	1.000×10^{-05}	3.346×10^{-06}	4.843×10^{-06}
	12.237[d]	1.647×10^{-03}	1.538×10^{-04}	8.277×10^{-05}	2.417×10^{-04}	1.703×10^{-04}	2.455×10^{-04}
	13.637[e]	1.641×10^{-06}	2.079×10^{-07}	1.674×10^{-07}	1.120×10^{-06}	2.246×10^{-07}	3.258×10^{-07}
	12.400[f]	6.935×10^{-04}	6.724×10^{-05}	3.776×10^{-05}	1.233×10^{-04}	7.419×10^{-05}	1.070×10^{-04}
^{294}Og	12.425[a]	7.741×10^{-05}	1.666×10^{-05}	1.051×10^{-05}	4.558×10^{-05}	1.773×10^{-05}	2.731×10^{-05}
	11.225[b]	5.495×10^{-02}	9.732×10^{-03}	4.557×10^{-03}	8.457×10^{-03}	1.060×10^{-02}	1.616×10^{-02}
	12.227[c]	2.518×10^{-04}	4.466×10^{-05}	2.670×10^{-05}	1.023×10^{-04}	4.770×10^{-05}	7.336×10^{-05}
	11.435[d]	1.614×10^{-02}	2.970×10^{-03}	1.458×10^{-03}	3.196×10^{-03}	3.222×10^{-03}	4.920×10^{-03}
	12.565[e]	3.835×10^{-05}	8.414×10^{-06}	5.521×10^{-06}	2.603×10^{-05}	8.931×10^{-06}	1.377×10^{-05}
	11.650[g]	4.770×10^{-03}	9.122×10^{-04}	4.708×10^{-04}	1.214×10^{-03}	9.850×10^{-04}	1.507×10^{-03}
^{290}Lv	11.124[a]	2.015×10^{-02}	4.388×10^{-03}	2.219×10^{-03}	5.284×10^{-03}	4.610×10^{-03}	7.437×10^{-03}
	10.634[b]	3.975×10^{-01}	7.929×10^{-02}	3.617×10^{-02}	5.781×10^{-02}	8.420×10^{-02}	1.349×10^{-01}
	11.110 [c]	3.720×10^{-02}	4.740×10^{-03}	2.390×10^{-03}	5.632×10^{-03}	4.982×10^{-03}	8.035×10^{-03}
	10.734[d]	2.126×10^{-01}	4.322×10^{-02}	2.011×10^{-02}	3.501×10^{-02}	4.580×10^{-02}	7.346×10^{-02}
	11.394[e]	4.245×10^{-03}	9.651×10^{-04}	5.195×10^{-04}	1.511×10^{-03}	1.008×10^{-03}	1.633×10^{-03}
	10.840 [g]	1.106×10^{-01}	2.288×10^{-02}	1.088×10^{-02}	2.069×10^{-02}	2.419×10^{-02}	3.886×10^{-02}
^{286}Fl	9.522 [a]	$1.332 \times 10^{+02}$	$2.671 \times 10^{+01}$	$1.107 \times 10^{+01}$	9.109×10^{00}	$2.797 \times 10^{+01}$	$4.615 \times 10^{+01}$
	9.782[b]	$2.067 \times 10^{+01}$	4.392×10^{00}	1.889×10^{00}	2.023×10^{00}	4.568×10^{00}	7.581×10^{00}
	9.993[c]	$1.218 \times 10^{+01}$	1.072×10^{00}	4.769×10^{-01}	6.244×10^{-01}	1.109×10^{00}	1.849×10^{00}
	10.332[d]	5.104×10^{-01}	1.209×10^{-01}	5.719×10^{-02}	1.013×10^{-01}	1.241×10^{-01}	2.085×10^{-01}
	9.662[e]	$4.838 \times 10^{+01}$	$1.001 \times 10^{+01}$	4.231×10^{00}	4.021×10^{00}	$1.045 \times 10^{+01}$	$1.729 \times 10^{+01}$
	10.190[g]	1.288×10^{00}	2.975×10^{-01}	1.370×10^{-01}	2.146×10^{-01}	3.064×10^{-01}	5.130×10^{-01}
^{282}Cn	9.481[a]	$2.654 \times 10^{+01}$	7.575×10^{00}	3.397×10^{00}	4.087×10^{00}	7.601×10^{00}	$1.311 \times 10^{+01}$
	10.191[b]	2.108×10^{-01}	6.805×10^{-02}	3.443×10^{-02}	7.788×10^{-02}	6.711×10^{-02}	1.180×10^{-01}
	10.163[c]	7.375×10^{-01}	8.072×10^{-02}	4.062×10^{-02}	8.989×10^{-02}	7.966×10^{-02}	1.400×10^{-01}
	9.731[d]	4.544×10^{00}	1.359×10^{00}	6.334×10^{-01}	9.645×10^{-01}	1.355×10^{00}	2.354×10^{00}
	9.671[e]	6.895×10^{00}	2.040×10^{00}	9.417×10^{-01}	1.357×10^{00}	2.037×10^{00}	3.533×10^{00}
^{278}Ds	10.359[a]	1.332×10^{-02}	5.617×10^{-03}	3.243×10^{-03}	1.176×10^{-02}	5.270×10^{-03}	9.764×10^{-03}
	10.179[b]	4.083×10^{-02}	1.686×10^{-02}	9.370×10^{-03}	2.985×10^{-02}	1.588×10^{-02}	2.926×10^{-02}
	10.280[c]	6.780×10^{-02}	9.044×10^{-03}	5.135×10^{-03}	1.761×10^{-02}	8.500×10^{-03}	1.571×10^{-02}
	10.129[d]	5.604×10^{-02}	2.299×10^{-02}	1.265×10^{-02}	3.883×10^{-02}	2.168×10^{-02}	3.990×10^{-02}
	10.659[e]	2.201×10^{-03}	9.573×10^{-04}	5.913×10^{-04}	2.624×10^{-03}	8.923×10^{-04}	1.668×10^{-03}
^{274}Hs	9.588[a]	4.050×10^{-01}	1.671×10^{-01}	9.123×10^{-02}	2.649×10^{-01}	1.520×10^{-01}	2.866×10^{-01}
	9.508[b]	6.995×10^{-01}	2.854×10^{-01}	1.536×10^{-01}	4.186×10^{-01}	2.601×10^{-01}	4.887×10^{-01}
	9.570[c]	1.708×10^{00}	1.880×10^{-01}	1.023×10^{-01}	2.930×10^{-01}	1.711×10^{-01}	3.223×10^{-01}
	9.628[d]	3.090×10^{-01}	1.282×10^{-01}	7.051×10^{-02}	2.112×10^{-01}	1.165×10^{-01}	2.200×10^{-01}
	9.698[e]	1.933×10^{-01}	8.098×10^{-02}	4.510×10^{-02}	1.426×10^{-01}	7.346×10^{-02}	1.391×10^{-01}
^{270}Sg	8.276[a]	$1.214 \times 10^{+03}$	$5.063 \times 10^{+02}$	$2.516 \times 10^{+02}$	$3.418 \times 10^{+02}$	$4.529 \times 10^{+02}$	$8.323 \times 10^{+02}$
	8.776[b]	$2.254 \times 10^{+01}$	$1.035 \times 10^{+01}$	5.438×10^{00}	$1.192 \times 10^{+01}$	9.125×10^{00}	$1.722 \times 10^{+01}$
	8.681[c]	$2.629 \times 10^{+02}$	$2.112 \times 10^{+01}$	$1.096 \times 10^{+01}$	$2.206 \times 10^{+01}$	$1.867 \times 10^{+01}$	$3.506 \times 10^{+01}$
	8.626[d]	$7.176 \times 10^{+01}$	$3.209 \times 10^{+01}$	$1.654 \times 10^{+01}$	$3.164 \times 10^{+01}$	$2.841 \times 10^{+01}$	$5.320 \times 10^{+01}$
	8.396[e]	$4.509 \times 10^{+02}$	$1.929 \times 10^{+02}$	$9.693 \times 10^{+01}$	$1.486 \times 10^{+02}$	$1.719 \times 10^{+02}$	$3.180 \times 10^{+02}$

[a] Q value calculated using mass excess taken from FRDM [27].
[b] Q value calculated using mass excess taken from KTUY [28].
[c] Q value calculated using mass excess taken from WS4+RBF [29].
[d] Q value calculated using mass excess taken from HFBCS [30].
[e] Q value calculated using mass excess taken from TFM [31].
[f] Q value taken from Ref. [8].
[g] Experimental Q value taken from Ref. [8].

is given as

$$\log_{10}(T_{1/2}) = (aZ + b)Q^{-1/2} + cZ + d + h_{\log}. \quad (19)$$

Here Z is the atomic number, and a, b, c, and d are adjustable parameters, given as $a = 1.661\ 75$, $b = -8.5166$, $c = -0.202\ 28$, and $d = -33.9069$. $h_{\log}$ is the hindrance factor for the nuclei with unpaired nucleons. The values of $h_{\log}$ for different combinations are, $h_{\log}^{e-e} = 0$, $h_{\log}^{o-e} = 0.772$, $h_{\log}^{e-o} = 1.066$, and $h_{\log}^{o-o} = 1.114$.

The details of the results obtained for the isotope $^{298}120$ is given in Table I. The difference in the Q value using different mass tables is evident from the table. For example, if we consider the isotope ^{286}Fl, the experimental Q value is 10.190 MeV. Using the FRDM, the Q value is given by 9.522 MeV. The KTUY mass table predicts the Q value as 9.782 MeV. With the mass table of WS4+RBF the value is 9.993 MeV. The HFBCS and TFM give the Q value for the same isotope as 10.332 MeV and 9.662 MeV respectively. The sensitivity of Q value to the mass model has been given by different theoretical studies [52,53,55–57]. Analyzing the values, it is clear that the discrepancies in the Q value increases while going in to the very heavy region. For example, if we consider $^{298}120$, the Q value taken from Ref. [8] is 12.400 MeV. The Q value using FRDM is 13.297 MeV. KTUY gives the Q value as 11.687 MeV. 13.039 MeV, 12.237 MeV, and 13.637 MeV are the Q values using WS4+RBF, HFBCS, and TF mass models respectively. While analyzing the Q values, it is seen that for all the isotopes under study, the predictions using the HFBCS mass model shows less deviation from the experimental values. Here, it should be noted that Ref. [8] does not give the experimental data on the Q values for the isotopes $^{298,299}120$. The changes in the values of half-lives with the Q values are also evident from the table. In the case of $^{298}120$, if we input the Q value with the FRDM mass table (13.297 MeV), the CPPMDN gives the half-life of the isotope as 7.938×10^{-06} s. If we consider the Q value with the KTUY mass table (11.687 MeV), the CPPMDN predicts the half-life of the same isotope as 3.491×10^{-02} s. That is, a difference in 1.61 MeV in the Q value will able to make four order differences in the prediction of half-lives. It is seen that the half-lives using all the theoretical formalisms agree well with each other.

For a better understanding, we have plotted the Q value verses mass number for the different isotopes in the decay chain and is given in Fig. 1. From the figure also, it is seen that the values predicted using HFBCS mass model will have better matching with the experimental results. Also, the Q values predicted using the macroscopic-microscopic models FRDM, WS4+RBF, and TFM follow the same trend. The average deviation between calculated and the experimental Q value is greater, whereas, using TFM. The logarithmic half-lives using CPPMDN versus mass number of the isotopes is plotted and is given in Fig. 2. The difference in predictions of half-lives for an isotopes using Q values calculated with different models can be clearly seen from the figure.

The predictions for the decay chain of the isotope $^{299}120$ are given in Table II. In this case also, we can see the difference between Q values using different mass models. As mentioned earlier, the difference is evident in the very

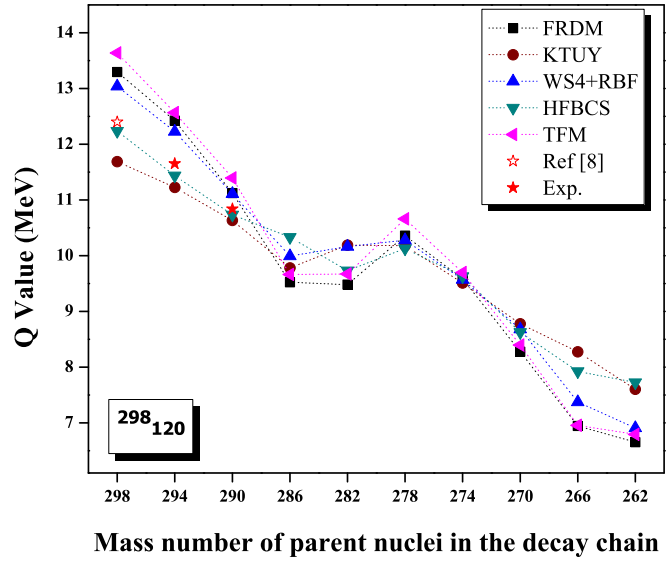

FIG. 1. Comparison of calculated Q values using five different mass models with the experimental values [8] for the isotopes in the decay chain of $^{298}120$.

heavy region. For the isotope $^{299}120$, the discrepancy in the calculation of Q value varies from 0.581 MeV (HFBCS) to 1.487 MeV (FRDM). The predictions using the HFBCS model agrees better with experimental results. The absolute value of discrepancy between experimental and theoretical Q value is less than 0.60 MeV for all the isotopes in the decay chain, while using the HFBCS mass model. From this analysis, it is clear that, the use of the HFBCS model will give better predictions on Q values as compared to the other widely used models, such as FRDM and WS4. Similar conclusions are also obtained by Sobiczewski and Litvinov [51], by analyzing different mass models. The Q value versus mass number

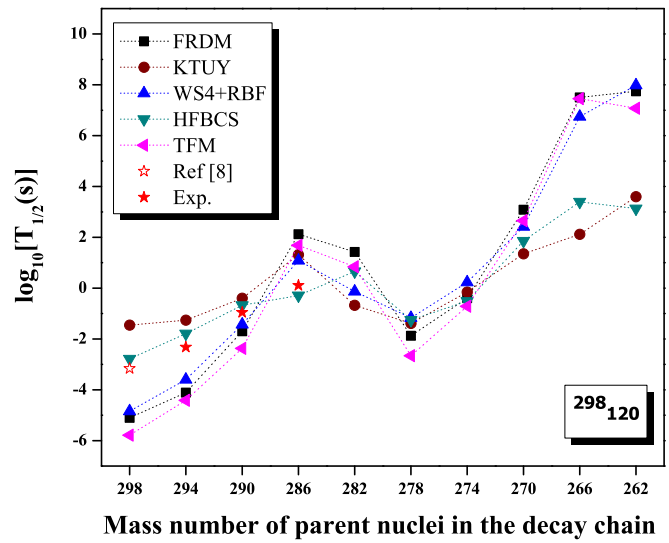

FIG. 2. Comparison of α decay half-lives (calculated using CPPMDN) with the Q values using five different mass models for the isotopes in the decay chain of $^{298}120$.

TABLE II. Calculated values of α-decay energies and half-lives for the isotopes in the decay chain of $^{299}120$ using five different mass models and six different theoretical formalisms, respectively.

		$T^{\alpha}_{1/2}$ (s)					
Parent nuclei	Q_{α} (MeV)	CPPMDN	Royer	UNIV	MBrown	AP	VSS
$^{299}120$	13.787[a]	6.503×10^{-07}	6.424×10^{-07}	8.875×10^{-08}	1.937×10^{-06}	1.295×10^{-06}	1.981×10^{-06}
	11.709[b]	2.246×10^{-02}	1.469×10^{-02}	1.145×10^{-03}	6.868×10^{-03}	4.616×10^{-02}	4.706×10^{-02}
	13.274[c]	6.792×10^{-06}	6.145×10^{-06}	7.246×10^{-07}	1.218×10^{-05}	1.368×10^{-05}	1.911×10^{-05}
	11.719[d]	2.122×10^{-02}	1.391×10^{-02}	1.087×10^{-03}	6.570×10^{-03}	4.361×10^{-02}	4.456×10^{-02}
	13.369[e]	4.354×10^{-06}	4.002×10^{-06}	4.857×10^{-07}	8.590×10^{-06}	8.745×10^{-06}	1.243×10^{-05}
	12.300[f]	8.755×10^{-04}	6.532×10^{-04}	5.876×10^{-05}	5.443×10^{-04}	1.788×10^{-03}	2.068×10^{-03}
^{295}Og	11.985[a]	2.111×10^{-03}	8.567×10^{-04}	8.334×10^{-05}	8.269×10^{-04}	3.086×10^{-03}	2.953×10^{-03}
	11.147[b]	2.689×10^{-01}	8.434×10^{-02}	6.759×10^{-03}	3.577×10^{-02}	3.722×10^{-01}	2.948×10^{-01}
	11.914[c]	3.120×10^{-03}	1.240×10^{-03}	1.185×10^{-04}	1.120×10^{-03}	4.541×10^{-03}	4.279×10^{-03}
	11.117[d]	3.231×10^{-01}	1.004×10^{-01}	7.995×10^{-03}	4.126×10^{-02}	4.464×10^{-01}	3.510×10^{-01}
	12.457[e]	1.713×10^{-04}	7.930×10^{-05}	8.735×10^{-06}	1.173×10^{-04}	2.571×10^{-04}	2.714×10^{-04}
	11.550[g]	2.446×10^{-02}	8.731×10^{-03}	7.646×10^{-04}	5.560×10^{-03}	3.485×10^{-02}	3.031×10^{-02}
^{291}Lv	11.074[a]	2.602×10^{-02}	3.071×10^{-02}	2.816×10^{-03}	1.961×10^{-02}	1.704×10^{-01}	1.153×10^{-01}
	10.496[b]	9.194×10^{-01}	9.712×10^{-01}	7.935×10^{-02}	3.417×10^{-01}	6.279×10^{00}	3.676×10^{00}
	11.130[c]	1.870×10^{-02}	2.230×10^{-02}	2.070×10^{-03}	1.505×10^{-02}	1.220×10^{-01}	8.369×10^{-02}
	10.816[d]	1.232×10^{-01}	1.386×10^{-01}	1.204×10^{-02}	6.822×10^{-02}	8.220×10^{-01}	5.222×10^{-01}
	11.366[e]	4.784×10^{-03}	5.922×10^{-03}	5.797×10^{-04}	5.023×10^{-03}	3.055×10^{-02}	2.216×10^{-02}
	10.740[g]	1.969×10^{-01}	2.182×10^{-01}	1.867×10^{-02}	9.932×10^{-02}	1.320×10^{00}	8.230×10^{-01}
^{287}Fl	9.452[a]	$2.142 \times 10^{+02}$	$2.173 \times 10^{+02}$	$1.738 \times 10^{+01}$	$4.042 \times 10^{+01}$	$2.375 \times 10^{+03}$	$8.849 \times 10^{+02}$
	9.664[b]	$4.580 \times 10^{+01}$	$4.872 \times 10^{+01}$	$4.008 \times 10^{+00}$	$1.161 \times 10^{+01}$	$4.985 \times 10^{+02}$	$1.980 \times 10^{+02}$
	9.777[c]	$2.056 \times 10^{+01}$	$2.252 \times 10^{+01}$	1.883×10^{00}	6.100×10^{00}	$2.227 \times 10^{+02}$	$9.143 \times 10^{+01}$
	9.814[d]	$1.587 \times 10^{+01}$	$1.746 \times 10^{+01}$	1.468×10^{00}	4.934×10^{00}	$1.707 \times 10^{+02}$	$7.087 \times 10^{+01}$
	9.564[e]	$9.420 \times 10^{+01}$	$9.793 \times 10^{+01}$	7.948×10^{00}	$2.079 \times 10^{+01}$	$1.033 \times 10^{+03}$	$3.984 \times 10^{+02}$
	10.020[g]	3.851×10^{00}	4.440×10^{00}	3.855×10^{-01}	1.574×10^{00}	$4.086 \times 10^{+01}$	$1.798 \times 10^{+01}$
^{283}Cn	9.181[a]	2.336×10^{02}	$3.054 \times 10^{+02}$	$2.705 \times 10^{+01}$	$7.312 \times 10^{+01}$	$4.567 \times 10^{+03}$	$1.314 \times 10^{+03}$
	9.633[b]	8.641×10^{00}	$1.238 \times 10^{+01}$	1.164×10^{00}	4.929×10^{00}	$1.606 \times 10^{+02}$	$5.314 \times 10^{+01}$
	9.850[c]	1.930×10^{00}	2.878×10^{00}	2.801×10^{-01}	1.444×10^{00}	$3.501 \times 10^{+01}$	$1.234 \times 10^{+01}$
	9.613[d]	9.947×10^{00}	$1.420 \times 10^{+01}$	1.332×10^{00}	5.532×10^{00}	$1.854 \times 10^{+02}$	$6.096 \times 10^{+01}$
	9.253[e]	$1.359 \times 10^{+02}$	$1.800 \times 0^{+02}$	$1.608 \times 10^{+01}$	$4.687 \times 10^{+01}$	$2.630 \times 10^{+03}$	$7.740 \times 10^{+02}$
	9.540[g]	$1.669 \times 10^{+01}$	$2.348 \times 10^{+01}$	2.179×10^{00}	8.447×10^{00}	$3.135 \times 10^{+02}$	$1.008 \times 10^{+02}$
^{279}Ds	9.629[a]	1.918×10^{00}	2.607×10^{00}	2.824×10^{-01}	1.767×10^{00}	$4.313 \times 10^{+01}$	$1.177 \times 10^{+01}$
	9.942[b]	8.741×10^{-01}	3.359×10^{-01}	3.841×10^{-02}	3.105×10^{-01}	5.075×10^{00}	1.517×10^{00}
	9.871[c]	$1.411 \times 10^{+00}$	5.300×10^{-01}	5.983×10^{-02}	4.572×10^{-01}	8.171×10^{00}	2.393×10^{00}
	9.911[d]	2.860×10^{-01}	4.073×10^{-01}	4.632×10^{-02}	3.657×10^{-01}	6.207×10^{00}	1.839×10^{00}
	9.921[e]	2.677×10^{-01}	3.820×10^{-01}	4.352×10^{-02}	3.463×10^{-01}	5.804×10^{00}	1.725×10^{00}
	9.700[g]	1.178×10^{00}	1.623×10^{00}	1.779×10^{-01}	1.182×10^{00}	$2.629 \times 10^{+01}$	7.327×10^{00}
^{275}Hs	9.398[a]	1.731×10^{00}	2.542×10^{00}	3.061×10^{-01}	2.321×10^{00}	$5.820 \times 10^{+01}$	$1.198 \times 10^{+01}$
	9.350[b]	2.427×10^{00}	3.521×10^{00}	4.208×10^{-01}	3.067×10^{00}	$8.180 \times 10^{+01}$	$1.659 \times 10^{+01}$
	9.295[c]	3.588×10^{00}	5.152×10^{00}	6.105×10^{-01}	4.248×10^{00}	$1.217 \times 10^{+02}$	$2.427 \times 10^{+01}$
	9.410[d]	1.591×10^{00}	2.334×10^{00}	2.816×10^{-01}	2.157×10^{00}	$5.325 \times 10^{+01}$	$1.101 \times 10^{+01}$
	9.610[e]	4.011×10^{-01}	6.089×10^{-01}	7.597×10^{-02}	6.830×10^{-01}	$1.309 \times 10^{+01}$	2.875×10^{00}
	9.300[g]	3.462×10^{00}	4.981×10^{00}	5.906×10^{-01}	4.127×10^{00}	$1.175 \times 10^{+02}$	$2.346 \times 10^{+01}$
^{271}Sg	8.526[a]	$1.516 \times 10^{+02}$	$2.760 \times 10^{+02}$	$3.400 \times 10^{+01}$	$1.801 \times 10^{+02}$	$1.094 \times 10^{+04}$	$1.335 \times 10^{+03}$
	8.669[b]	$4.922 \times 10^{+01}$	$9.245 \times 10^{+01}$	$1.157 \times 10^{+01}$	$7.005 \times 10^{+01}$	$3.491 \times 10^{+03}$	$4.483 \times 10^{+02}$
	8.646[c]	$5.887 \times 10^{+01}$	$1.097 \times 10^{+02}$	$1.369 \times 10^{+01}$	$8.117 \times 10^{+01}$	$4.172 \times 10^{+03}$	$5.316 \times 10^{+02}$
	8.409[d]	$3.889 \times 10^{+02}$	$6.943 \times 10^{+02}$	$8.453 \times 10^{+01}$	$3.995 \times 10^{+02}$	$2.867 \times 10^{+04}$	$3.353 \times 10^{+03}$
	8.619[e]	$7.270 \times 10^{+01}$	$1.353 \times 10^{+02}$	$1.684 \times 10^{+01}$	$9.735 \times 10^{+01}$	$5.198 \times 10^{+03}$	$6.558 \times 10^{+02}$
	8.540[g]	$1.356 \times 10^{+02}$	$2.478 \times 10^{+02}$	$3.056 \times 10^{+01}$	$1.641 \times 10^{+02}$	$9.774 \times 10^{+03}$	$1.199 \times 10^{+03}$

[a] Q value calculated using mass excess taken from FRDM [27].
[b] Q value calculated using mass excess taken from KTUY [28].
[c] Q value calculated using mass excess taken from WS4+RBF [29].
[d] Q value calculated using mass excess taken from HFBCS [30].
[e] Q value calculated using mass excess taken from TFM [31].
[f] Q value taken from Ref. [8].
[g] Experimental Q value taken from Ref. [8].

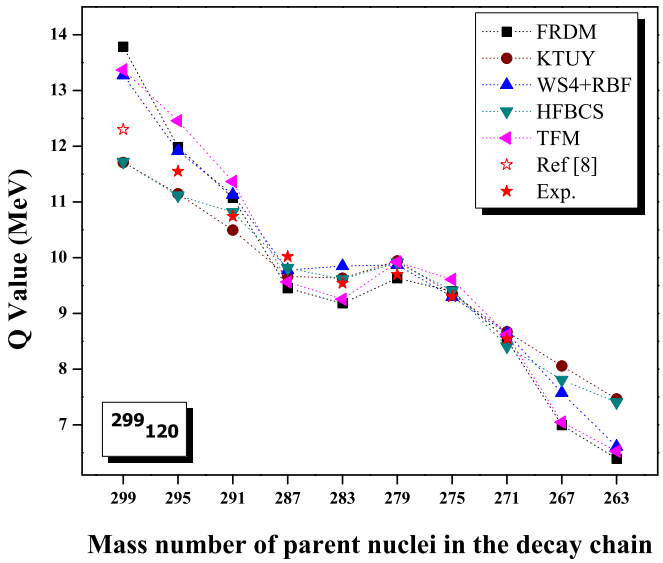

FIG. 3. Comparison of calculated Q values using five different mass models with the experimental values [8] for the isotopes in the decay chain of $^{299}120$.

plot for $^{299}120$ is given in Fig. 3. As in the case of $^{298}120$, predictions using FRDM, WS4+RBF, and TFM follow the same trend. The average deviation from experimental Q value is greater, while using TFM. The logarithmic half-lives versus mass number plot for the decay chain of the same isotope is given in Fig. 4. We can see that the change in the Q value around 2 MeV will make about five orders of difference in the calculation of decay half-lives.

To understand about the length of the α-decay chain of the isotopes under study, we have calculated the spontaneous fission half-lives using the shell-effect-dependent formula. The shell-effect-dependent formula is proved to give good results

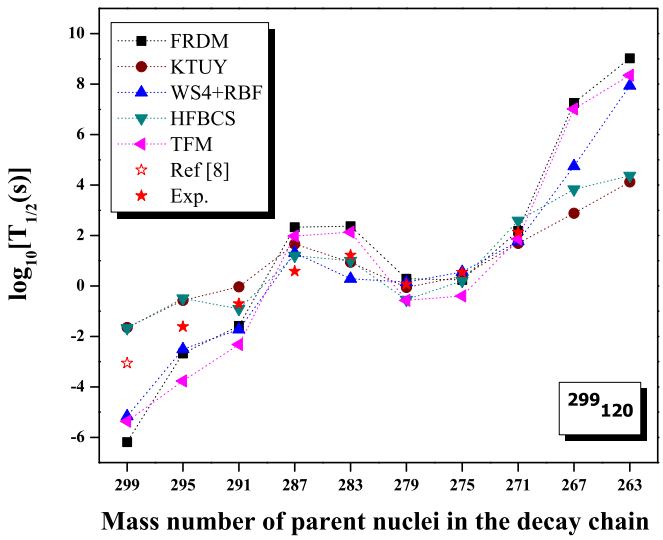

FIG. 4. Comparison of α decay half-lives (calculated using CPPMDN) with the Q values using five different mass models for the isotopes in the decay chain of $^{299}120$.

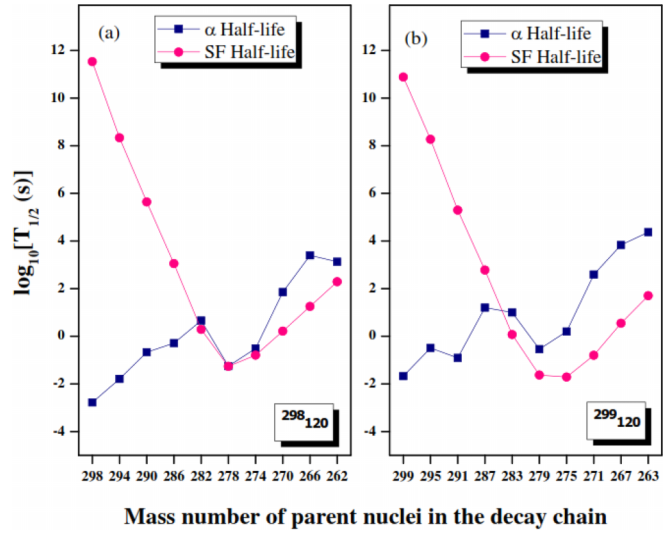

FIG. 5. Comparison of calculated α decay half-lives with the corresponding spontaneous fission half-lives for the isotopes (a) $^{298}120$, and (b) $^{299}120$.

for the spontaneous fission half-lives in the superheavy region [40]. The formula is given by

$$\log_{10}(T_{1/2}/\mathrm{yr}) = a\frac{Z^2}{A} + b\left(\frac{Z^2}{A}\right)^2 + c\left(\frac{N-Z}{N+Z}\right) + d\left(\frac{N-Z}{N+Z}\right)^2 + eE_{\mathrm{shell}} + f, \quad (20)$$

where $a = -43.252\ 03$, $b = 0.491\ 92$, $c = 3674.3927$, $d = -9360.6$, $e = 0.8930$, and $f = 578.560\ 58$. E_{shell} is the shell correction energy taken from Ref. [27].

The decay mode of each isotope in the chain is predicted by comparing its α half-life with the corresponding spontaneous fission half-life. If the α half-life is less than spontaneous fission half-life, then the isotope will decay via α decay. The α half-lives calculated with CPPMDN by inputting the Q values using HFBCS is used for the comparison and is given in Fig. 5. The result for the isotope $^{298}120$ is given in Fig. 5(a). It is seen that the isotope will decay via a 4α chain followed by spontaneous fission. It is in agreement with the results of Oganessian *et al.* [8]. In the case of $^{299}120$ [Fig. 5(b)], the theoretical predictions slightly differ from the observations of Oganession *et al.* [8]. Theoretically we have predicted 4α chain from $^{299}120$, followed by spontaneous fission. But according to Oganessian *et al.* [8] $^{299}120$ may exhibit an 8α chain. Here, it should be noted that, the daughter nuclei in the 5th position of the decay chain of $^{299}120$, that is, ^{279}Ds will have 90% chances to decay via spontaneous fission [8]. This shows an inconsistency in the mode of decay of $^{299}120$. So we have to look forward for further experimental details about the decay chain of $^{299}120$.

IV. CONCLUSIONS

The α-decay properties of the isotopes $^{298}120$ and $^{299}120$ are extensively studied in the present paper. The Q values

of the isotopes in the decay chain are calculated using five different mass models, including FRDM, KTUY, WS4+RBF, HFBCS, and TFM. α half-lives of the isotopes are calculated using CPPMDN. For a theoretical comparison of decay half-lives, we have used the analytical formula of Royer, UNIV, MBrown formula, AP formula, and the VSS formula. The length of the decay chain of these isotopes is predicted by comparing the α half-lives calculated using CPPMDN with the spontaneous fission half-lives using shell-effect-dependent formula.

The discrepancies in the calculation of Q value using different mass models are evident from the paper. Models of same nature will give the same trend in the prediction of the Q value. The purely microscopic HFBCS mass model give better prediction on the Q values as compared to the widely used models, such as FRDM. The α-decay half-lives calculated using all the theoretical formalisms agree well each other. For the same isotope, a 1-MeV difference in the calculation of the Q value will make several orders of differences in the prediction of half-lives.

By comparing the α half-lives with the corresponding spontaneous fission half-lives, it is seen that the isotopes $^{298}120$ and $^{299}120$ will decay via 4α chain followed by spontaneous fission. Since the half-lives are within the experimental limit, it may be possible to detect these isotopes via their α-decay chain. We hope that our studies will be helpful in the future experimental investigations for the isotopes of $Z = 120$.

[1] U. Mosel and W. Greiner, Z. Phys. **222**, 261 (1969).

[2] S. G. Nilsson, C. F. Tsang, A. Sobiczewski, Z. Szymański, S. Wycech, C. Gustafson, I.–L. Lamm, P. Möller, and B. Nilsson, Nucl. Phys. **A131**, 1 (1969).

[3] H. Meldner, Ark. Fys. **36**, 593 (1967).

[4] W. D. Myers and W. J. Swiatecki, Ark. Fys. **36**, 343 (1967).

[5] A. Sobiczewski, F. A. Gareev, and B. N. Kalinkin, Phys. Lett. **22B**, 500 (1966).

[6] S. Hofmann and G. Münzenberg, Rev. Mod. Phys. **72**, 733 (2000).

[7] Yu. Ts. Oganessian, J. Phys. G: Nucl. Part. Phys. **34**, R165 (2007).

[8] Yu. Ts. Oganessian, V. K. Utyonkov, Yu. V. Lobanov, F. Sh. Abdullin, A. N. Polyakov, R. N. Sagaidak, I. V. Shirokovsky, Yu. S. Tsyganov, A. A. Voinov, A. N. Mezentsev, V. G. Subbotin, A. M. Sukhov, K. Subotic, V. I. Zagrebaev, S. N. Dmitriev, R. A. Henderson, K. J. Moody, J. M. Kenneally, J. H. Landrum, D. A. Shaughnessy, M. A. Stoyer, N. J. Stoyer, and P. A. Wilk, Phys. Rev. C **79**, 024603 (2009).

[9] S. Hofmann, S. Heinz, R. Mann, J. Maurer, G. Münzenberg, S. Antalic, W. Barth, H. G. Burkhard, L. Dahl, K. Eberhardt, R. Grzywacz, J. H. Hamilton, R. A. Henderson, J. M. Kenneally, B. Kindler, I. Kojouharov, R. Lang, B. Lommel, K. Miernik, D. Miller, K. J. Moody, K. Morita, K. Nishio, A. G. Popeko, J. B. Roberto, J. Runke, K. P. Rykaczewski, S. Saro, C. Scheidenberger, H. J. Schött, D. A. Shaughnessy, M. A. Stoyer, P. Thörle-Pospiech, K. Tinschert, N. Trautmann, J. Uusitalo, and A. V. Yeremin, Eur. Phys. J. A **52**, 180 (2016).

[10] K. V. Novikov, E. M. Kozulin, G. N. Knyazheva, I. M. Itkis, A. V. Karpov, M. G. Itkis, I. N. Diatlov, M. Cheralu, B. Gall, Z. Asfari, N. I. Kozulina, D. Kumar, I. V. Pchelintsev, V. N. Loginov, A. E. Bondarchenko, P. P. Singh, I. V. Vorobiev, S. Heinz, W. H. Trzaska, E. Vardaci, N. Tortorelli, C. Borcea, and I. Harca, Bull. Russ. Acad. Sci.: Phys. **84**, 495 (2020).

[11] H. M. Albers, J. Khuyagbaatar, D. J. Hinde, I. P. Carter, K. J. Cook, M. Dasgupta, Ch. E. Düllmann, K. Eberhardt, D. Y. Jeung, S. Kalkal, B. Kindler, N. R. Lobanov, B. Lommel, C. Mokry, E. Prasad, D. C. Rafferty, J. Runke, K. Sekizawa, C. Sengupta, C. Simenel, E. C. Simpson, J. F. Smith, P. Thörle-Pospiech, N. Trautmann, K. Vo-Phuoc, J. Walshe, E. Williams, and A. Yakushev, Phys. Lett. B **808**, 135626 (2020).

[12] J. Khuyagbaatar, A. Yakushev, Ch. E. Düllmann, D. Ackermann, L.-L. Andersson, M. Asai, M. Block, R. A. Boll, H. Brand, D. M. Cox, M. Dasgupta, X. Derkx, A. Di Nitto, K. Eberhardt, J. Even, M. Evers, C. Fahlander, U. Forsberg, J. M. Gates, N. Gharibyan, P. Golubev, K. E. Gregorich, J. H. Hamilton, W. Hartmann, R.-D. Herzberg, F. P. Heßberger, D. J. Hinde, J. Hoffmann, R. Hollinger, A. Hübner, E. Jäger, B. Kindler, J. V. Kratz, J. Krier, N. Kurz, M. Laatiaoui, S. Lahiri, R. Lang, B. Lommel, M. Maiti, K. Miernik, S. Minami, A. K. Mistry, C. Mokry, H. Nitsche, J. P. Omtvedt, G. K. Pang, P. Papadakis, D. Renisch, J. B. Roberto, D. Rudolph, J. Runke, K. P. Rykaczewski, L. G. Sarmiento, M. Schädel, B. Schausten, A. Semchenkov, D. A. Shaughnessy, P. Steinegger, J. Steiner, E. E. Tereshatov, P. Thörle-Pospiech, K. Tinschert, T. Torres De Heidenreich, N. Trautmann, A. Türler, J. Uusitalo, M. Wegrzecki, N. Wiehl, S. M. Van Cleve, and V. Yakusheva, Phys. Rev. C **102**, 064602 (2020).

[13] E. M. Kozulin, G. N. Knyazheva, I. M. Itkis, M. G. Itkis, A. A. Bogachev, L. Krupa, T. A. Loktev, S. V. Smirnov, V. I. Zagrebaev, J. Aysto, W. H. Trzaska, V. A. Rubchenya, E. Vardaci, A. M. Stefanini, M. Cinausero, L. Corradi, E. Fioretto, P. Mason, G. F. Prete, R. Silvestri, S. Beghini, G. Montagnoli, F. Scarlassara, F. Hanappe, S. V. Khlebnikov, J. Kliman, A. Brondi, A. Di Nitto, R. Moro, N. Gelli, and S. Szilner, Phys. Lett. B **686**, 227 (2010).

[14] K. V. Novikov, E. M. Kozulin, G. N. Knyazheva, I. M. Itkis, M. G. Itkis, A. A. Bogachev, I. N. Diatlov, M. Cheralu, D. Kumar, N. I. Kozulina, A. N. Pan, I. V. Pchelintsev, I. V. Vorobiev, W. H. Trzaska, S. Heinz, H. M. Devaraja, B. Lommel, E. Vardaci, S. Spinosa, A. Di Nitto, A. Pulcini, S. V. Khlebnikov, Pushpendra P. Singh, Rudra N. Sahoo, B. Gall, Z. Asfari, C. Borcea, I. Harca, and D. M. Filipescu, Phys. Rev. C **102**, 044605 (2020).

[15] C. Nithya and K. P. Santhosh, Nucl. Phys. **A1020**, 122400 (2022).

[16] S. A. Seyyedi, Int. J. Mod. Phys. E **29**, 2050025 (2020).

[17] Z. H. Liu and J. D. Bao, Phys. Rev. C **80**, 054608 (2009).

[18] A. Ansari and N. Ghahramany, Iran. J. Sci. Technol. Trans. Sci **43**, 291 (2019).

[19] G. G. Adamian,N. V. Antonenko, H. Lenske, and L. A. Malov, Phys. Rev. C **101**, 034301 (2020).

[20] G. Saxena, M. Kumawat, S. S. Singh, and M. Aggarwal, Int. J. Mod. Phys. E **28**, 1950008 (2019).

[21] K. P. Santhosh and B. Priyanka, Phys. Rev. C **90**, 054614 (2014).

[22] A. Sobiczewski, Act. Phys. Pol., B **42**, 1871 (2011).
[23] K. Sekizawa and K. Hagino, Phys. Rev. C **99**, 051602(R) (2019).
[24] D. N. Poenaru and R. A. Gherghescu, Phys. Rev. C **97**, 044621 (2018).
[25] E. Olsen and W. Nazarewicz, Phys. Rev. C **99**, 014317 (2019).
[26] F. Li, L. Zhu, Z.-H. Wu, X.-B. Yu, J. Su, and C- C. Guo, Phys. Rev. C **98**, 014618 (2018).
[27] P. Moller, A. J. Sierk, T. Ichikawa, and H. Sagawa, At. Data Nucl. Data Tables **109**, 1 (2016).
[28] H. Koura, T. Tachibana, M. Uno, and M. Yamada, Prog. Theor. Phys. **113**, 305 (2005).
[29] N. Wang, M. Liu, X. Wu, and J. Meng, Phys. Lett. B **734**, 215 (2014).
[30] S. Goriely, F. Tondeur, and J. M. Pearson, At. Data Nucl. Data Tables **77**, 311 (2001).
[31] W. D. Myers and W. J. Swiatecki, Nucl. Phys. A **601**, 141 (1996).
[32] K. P. Santhosh, S. Sabina, and G. J. Jayesh, Nucl. Phys. A **850**, 34 (2011).
[33] G. Royer, J. Phys. G: Nucl. Part. Phys. **26**, 1149 (2000).
[34] D. N. Poenaru, R. A. Gherghescu, and W. Greiner, Phys. Rev. C **83**, 014601 (2011).
[35] D. N. Poenaru, R. A. Gherghescu, and W. Greiner, Phys. Rev. C **85**, 034615 (2012).
[36] A. I. Budaca, R. Budaca, and I. Silisteanu, Nucl. Phys. A **951**, 60 (2016).
[37] D. T. Akrawy and D. N. Poenaru, J. Phys. G: Nucl. Part. Phys. **44**, 105105 (2017).
[38] V. E. Viola, Jr. and G. T. Seaborg, and J. Inorg, Nucl. Chem. **28**, 741 (1966).
[39] A. Sobiczewski, Z. Patyk, and S. Ćwiok, Phys. Lett. B **224**, 1 (1989).
[40] K. P. Santhosh and C. Nithya, Phys. Rev. C **94**, 054621 (2016).
[41] C. Y. Wong, Phys. Rev. Lett. **31**, 766 (1973).
[42] N. Malhotra and R. K. Gupta, Phys. Rev. C **31**, 1179 (1985).
[43] R. K. Gupta, M. Balasubramaniam, R. Kumar, N. Singh, M. Manhas, and W. Greiner, J. Phys. G: Nucl. Part. Phys. **31**, 631 (2005).
[44] A. J. Baltz and B. F. Bayman, Phys. Rev. C **26**, 1969 (1982).
[45] Y. J. Shi and W. J. Swiatecki, Nucl. Phys. A **464**, 205 (1987).
[46] D. N. Poenaru, M. Ivascu, A. Sandulescu, and W. Greiner, Phys. Rev. C **32**, 572 (1985).
[47] R. C. Nayak and L. Satpathy, At. Data Nucl. Data Tables **98**, 616 (2012).
[48] S. Liran, A. Marinov, and N. Zeldes, arXiv:nucl-th/0102055.
[49] Y. Aboussir, A. K. Dutta, and F. Tondeur, At. Data Nucl. Data Tables **61**, 127 (1995).
[50] J. Duflo and A. P. Zuker, Phys. Rev. C **52**, R23(R) (1995).
[51] A. Sobiczewski and Y. A. Litvinov, Phys. Rev. C **89**, 024311 (2014).
[52] Y. Z. Wang, S. J. Wang, Z. Y. Hou, and J. Z. Gu, Phys. Rev. C **92**, 064301 (2015).
[53] V. Y. Denisov and A. A. Khudenko, Phys. Rev. C **79**, 054614 (2009).
[54] K. N. Huang, M. Aoyagi, M. H. Chen, B. Crasemann, and H. Mark, At. Data Nucl. Data Tables **18**, 243 (1976).
[55] K. P. Santhosh and C. Nithya, Phys. Rev. C **97**, 044615 (2018).
[56] A. Sobiczewski, J. Phys. G: Nucl. Part. Phys. **43**, 095106 (2016).
[57] A. Sobiczewski, Phys. Rev. C **94**, 051302(R) (2016).